Near-band-gap photoluminescence of Si-Ge alloys

J. Weber and M. I. Alonso
Max-Planck-Institut für Festkörperforschung, Heisenbergstrasse 1, Postfach 80 06 65, D-7000 Stuttgart 80, Federal Republic of Germany
(Received 6 March 1989)

The low-temperature near-band-gap photoluminescence of $Si_{1-x}Ge_x$ is studied over the whole composition range $0 \leq x \leq 1$. We identify free- and bound-exciton processes and determine the properties of momentum-conserving phonons. From our results we determine the low-temperature band gap of the alloys. Analytical expressions are derived for the X and L bands: $E_{gx}^{X}(x)=1.155-0.43x+0.206x^2$ eV; $E_{gx}^{L}(x)=2.010-1.270x$ eV. The intensity and the linewidth of the various excitonic transitions are found to depend only on the statistical alloy fluctuations. No preferential clustering of Si and Ge atoms is detected.

I. INTRODUCTION

The elemental semiconductors silicon and germanium form a continuous series of disordered alloys. A detailed understanding of the properties of the Si-Ge alloys is a prerequisite for successful device applications. The manipulation of semiconductor materials by the growth of superstructures leads to new and sometimes unexpected semiconductor properties. Examples are the enhanced mobility[1] and the appearance of new direct optical transitions in strained Si-Ge superlattices.[2,3] In this paper, we concentrate on the bulk properties of Si-Ge alloys. The object is to study and to reevaluate fundamental parameters in the alloys; for example, the energy of the indirect band gap, the properties of momentum-conserving (MC) phonons, and the importance of alloy fluctuations. We use the photoluminescence (PL) technique to characterize the samples and to study their properties. Luminescence measurements of Si-Ge alloys have been reported only for Si- or Ge-rich alloys. Free-exciton (FE) and bound-exciton (BE) luminescence, donor-acceptor–pair recombination, and electron-hole droplets were studied in Ge-rich alloys.[4–6] On the other hand, high-resolution spectra of FE and BE recombination, as well as deep luminescence centers, were reported from Si-rich alloys.[7,8] In this paper, we present a high-resolution PL investigation of Si-Ge alloys over the whole composition range.

The paper is organized as follows. In Sec. II, the experimental conditions and the sample descriptions are given. Section III deals with the experimental results of the PL measurements and the PL lines are identified. In Sec. IV, we derive the low-temperature band gap of alloys from the PL data, discuss the phonon structure in the alloys, and give evidence for a purely random distribution of the Si and Ge atoms in our samples. A summary of the results is given in Sec. V.

II. EXPERIMENTAL

A. Photoluminescence

The photoluminescence spectra of Si-Ge samples are measured in a conventional PL setup. The luminescence is excited by the above-band-gap light of different Ar^+-laser or Kr^+-laser lines. The excitation power varies between ~ 5 and 100 mW/mm^2. The samples are mounted in a glass cryostat, immersed in liquid helium, or in a temperature-controlled cryostat (Leybold), which allows us to vary the sample temperature between 1.6 K and room temperature.

Photoluminescence signals are analyzed by a 1-m grating monochromator (Spex 1702) and detected by a liquid-nitrogen-cooled Ge detector (North Coast). The signals are processed in standard lock-in technique. Data storage, lock-in, and monochromator settings are controlled by a desktop computer.

B. Sample preparation

In the present study we use $Si_{1-x}Ge_x$ alloy samples grown by various methods. Bulk Si-Ge alloys are cut from polycrystalline ingots with fairly large grains, which were prepared by a zone-leveling technique.[9] The nominally undoped samples show p-type conductivity with free-hole concentrations of the order of 10^{15} cm^{-3} at room temperature. A few samples are As doped up to a concentration of 3×10^{17} free electrons/cm^3. The samples are well characterized and have been previously used for electroreflectance[10] and Raman scattering[11] measurements.

The near-band-gap photoluminescence data presented here correspond mainly to these samples, for reasons to be discussed later. We also present the results of measurements performed on layers of Si-Ge alloys grown on Si substrates by liquid-phase (LPE) and vapor-phase (VPE) epitaxy. The LPE layers are grown from In or Sn solutions, as described in Ref. 12, whereas the VPE samples are crystallized from a Ge-Si chalcogen vapor phase, in an analogous way to that used for Si growth.[13] Both LPE and VPE layers have thicknesses between 0.3 and 20 μm.

C. Determination of the alloy composition

The compositions for the different sets of samples were determined employing diverse techniques. The alloy

 ©1989 The American Physical Society

compositions of the bulk samples already investigated in Refs. 10 and 11 were determined from density measurements.[9] For a few of the LPE layers we calculate the composition from the lattice constant,[9] which was measured by x-ray diffraction. In all cases we checked by Raman measurements that the layers were not strained.[14] The VPE samples had nominal compositions calculated from the amounts of Si and Ge contained in the vapor phase.

All samples used in this study are characterized by spectral ellipsometry, which gives the energies of the direct interband electronic transitions in the material. The electronic gaps vary linearly with the composition in the Si-Ge alloy system.[10] In particular, the E_1 gap gives rise to a large structure whose energy varies by about 1.2 eV from Ge to Si and, therefore allows a rapid and accurate determination of the alloy composition. We used an interpolation of the E_1 energy between Si and Ge, according to Ref. 15, to obtain the composition of our samples. The E_1 energy is found by fitting the numerically calculated second derivative of the ellipsometric spectrum with an analytical two-dimensional critical point line shape (for details see Ref. 15). The accuracy of our fitted E_1 energy is typically between 5 and 10 meV, which implies an accuracy in composition better than 0.5 to 1.0 at. % Ge. The "optical" compositions so obtained are in good agreement with the x-ray-diffraction data where these are available, with discrepancies of, at most, 3%. In the presentation of our measurements we always use the optical composition x to describe the alloy composition.

The homogeneity of the samples critically depends on the growth process of the samples. In the polycrystalline samples, the typical energy changes in the luminescence lines for different excitation spots on the samples correspond to variations in the composition of different grains of not more than 3 at. % Ge. In the LPE or VPE layers, no shift of luminescence lines was found for different excitation spots, although a grading of the composition in depth could be detected by x-ray-diffraction measurements.[16] Apparently the excitons diffuse to the regions of lowest band gap and recombine. In some LPE-grown samples with high dislocation densities, the excitonic diffusion is hindered and recombination occurs in the excitation volume of the laser. Only in these LPE samples could we detect small shifts of the luminescence lines due to variations in the alloy composition.

III. EXPERIMENTAL RESULTS AND IDENTIFICATION OF THE PHOTOLUMINESCENCE LINES

A. General features of the photoluminescence spectra

In this section, we present PL spectra of Si-Ge alloy samples and give a labeling of the low-temperature near-band-gap PL lines, which will be discussed in detail later.

In the course of our study of Si-Ge alloys, we found that the near-band-gap low-temperature PL spectra of differently grown samples show the same gross features. However, our polycrystalline samples exhibit, in general, spectra of superior quality compared to the samples grown by the LPE and VPE techniques. The optical transitions in the bulk Si-Ge samples have a much smaller linewidth (in most cases by a factor of, at least, 3 to 5) compared to the optical transitions in the LPE layer. In addition, the intensity of the near-band-gap PL, in the LPE samples, is always very weak due to strong dislocation related PL bands.[17] Samples grown by VPE also show small linewidth optical transitions; however, these lines are usually superposed on very intense broad optical transitions of unknown origin.

In the presentation of our results, we will primarily focus on the PL spectra from the bulk samples. Only for the discussion of certain aspects, will spectra from the LPE and VPE samples be presented. The low-temperature PL spectra of lightly doped Si or Ge crystals are dominated by the optical recombination of bound excitons (BE). Due to the indirect nature in momentum space of the Si and Ge band gaps, the radiative recombination of an electron-hole pair within the bound-exciton complexes involves the creation of a phonon with a certain k value to conserve momentum during the optical process. However, it is also possible for the bound electron-hole pair to recombine without phonon participation. The impurity itself transfers the momentum in this so-called no-phonon (NP) transition. Such a transition is more likely to occur for deeper impurities with their larger spread of wave functions in k space. A typical low-temperature PL spectrum in Si and Ge doped with shallow impurities consists of the bound-exciton NP transitions and their phonon replicas at lower energies.[18] The intensity ratios of the NP line to the phonon replicas depend strongly on the binding energy and the type of impurity (donor, acceptor) and are different for Si and Ge. In general, the NP lines are weak, and increase in intensity with the binding energy of the complex. In Si, coupling to TO phonons is strongest followed by the coupling to TA phonons. In Ge, LA- and LO-phonon replicas of the BE's are favored.

We find a smooth variation of the characteristic PL features in the Si-Ge samples as the composition is varied. Figure 1 gives a few examples of the low-temperature near-band-gap photoluminescence for different compositions. The sample temperature in all measurements is $T=4.2$ K and the excitation is by the $\lambda=514$ nm line of an Ar^+ laser.

All spectra in Fig. 1 exhibit a simple, almost identical structure. We label the lines X with an upper index to characterize the optical transitions in more detail: NP, TA, and TO. For optical transitions, without the creation of a phonon, we use NP, and with the participation of a momentum-conserving (MC) phonon, we use TA, or TO. The subscript for the phonon lines (Ge-Ge, Si-Ge, Si-Si) specifies a distinct phonon in the alloys. A detailed discussion of the labeling will be given in the following sections.

For a description of the Si-Ge alloy spectra, we will start with the Si-rich sample $Si_{0.92}Ge_{0.08}$. The spectrum of this sample, displayed in Fig. 1, resembles those spectra found in crystalline Si. Differences are the energetic

position of the lines and their increased linewidth. In pure Si the NP transition of the BE's is roughly 30 meV higher in energy. This shift of the X^{NP} line is due to the reduced band gap in the alloy and will be discussed in more detail in Sec. IV. The $X^{TO}_{Si\text{-}Si}$ line appears at exactly the energy difference of the TO phonon in Si (58 meV) from the X^{NP} line.[19] In addition, the small shoulder on the low-energy side of the NP transition can be identified with the MC TA-phonon replica in silicon. Towards lower energies several weak two-phonon transitions can be detected.

The halfwidths of the lines (~ 7 meV for the X^{NP} transitions) are much larger than those of the BE transitions in silicon ($\lesssim 0.3$ meV). With higher Ge content in the alloy the lines become sharper and more structure is found in the phonon replicas.

We detect in the alloys phonon energies that are close to those of pure germanium and silicon, e.g., $X^{TO}_{Ge\text{-}Ge}$ and $X^{TO}_{Si\text{-}Si}$, but also phonons typical for the alloy ($X^{TO}_{Si\text{-}Ge}$).

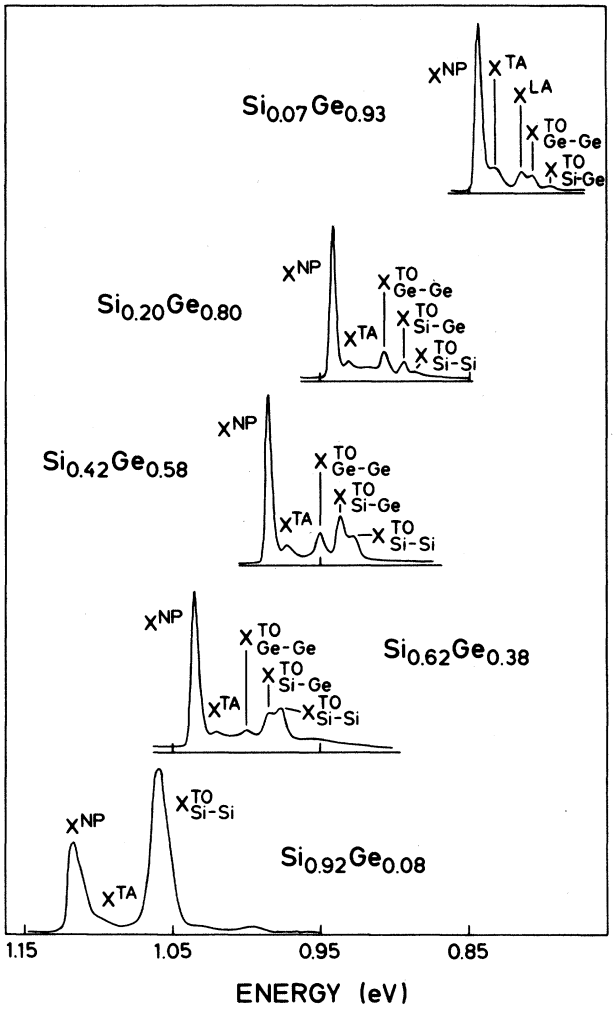

FIG. 1. Near-band-gap photoluminescence spectra for several bulk Si-Ge samples. The optical transitions are named X^j_i where j gives the type of transition (no-phonon or phonon participation) and i specifies the nature of the phonon.

Clearly, changes in the energetic position of the spectra and variations in the relative intensities of the line occur with increasing composition.

B. Identification of the free-exciton recombination

We have investigated the temperature dependence of the PL spectra of Si-Ge samples to identify the nature of the optical transitions. Figure 2 shows that as the temperature is increased the line labeled X^{NP} thermalizes with respect to the line labeled $(FE)^{NP}$. Above 12 K X^{NP} is no longer detectable and $(FE)^{NP}$ exhibits a shape characteristic of free-exciton (FE) recombination. The line shape of the FE line is easily fitted to the well-known expression[20]

$$I(E)\sim(E-E_{gx})^{1/2}\exp\left[\frac{E-E_{gx}}{kT}\right], \tag{1}$$

with $I(E)$ being the luminescence intensity at photon energy E, E_{gx} the excitonic band gap, and T the temperature. The fit temperature T obtained always agrees within 2 K with the bath temperature. However, in most samples a proper fit of the FE line shape was not possible because the intensity of the FE recombination was too weak. An example of such a spectrum is given in Fig. 3.

We identify the line labeled FE^{NP} due to its thermal behavior, as resulting from no-phonon FE recombination. The excitonic NP luminescence is greatly enhanced in the alloys, since the statistical distribution of the Si and Ge atoms can act as momentum-conserving scattering centers. We detect TA-, LA-, and TO-phonon replicas of the FE recombination, their intensities being dependent upon the composition.

The $(FE)^{NP}$ luminescence and its phonon replicas were first reported for Ge-rich alloys in Ref. 5. In low-doped Si-rich Si-Ge alloys, Mitchard and McGill identified the $(FE)^{NP}$ transitions. In their low-doped samples, the

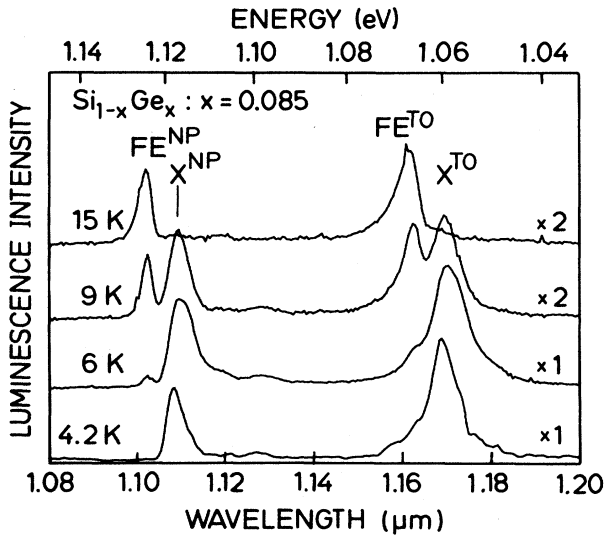

FIG. 2. Photoluminescence spectra of a bulk $Si_{1-x}Ge_x$ ($x=0.085$) sample at different temperatures.

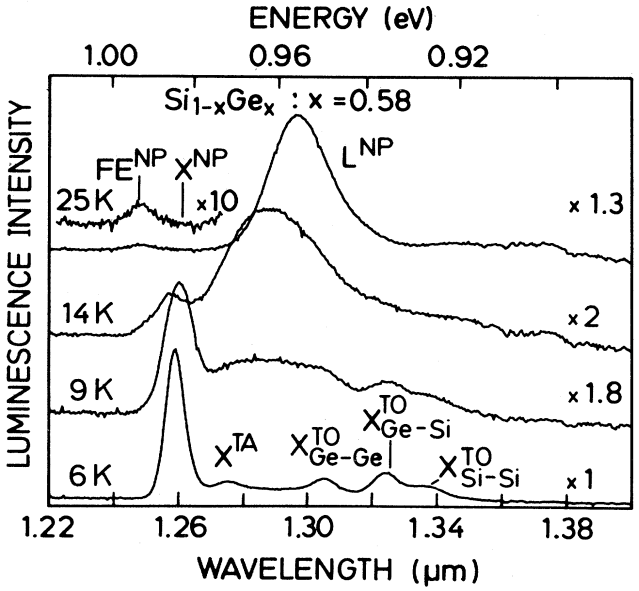

FIG. 3. Photoluminescence spectra of a bulk $Si_{1-x}Ge_x$ ($x=0.58$) sample at different temperatures.

$(FE)^{NP}$ was found even at 1.9 K.[7] A shift of the $(FE)^{NP}$ line towards smaller energies was detected at these temperatures and interpreted as due to the weak binding of excitons to alloy fluctuations.

All our samples have apparently much higher impurity concentrations because we can detect the FE luminescence only at higher temperatures $T \gtrsim 5$ K. At this temperature, the thermal ionization of BE's into FE's results in an increase in the FE luminescence intensity. In our samples the FE luminescence shows no shift in energy with sample temperature.

In a few of our LPE samples we can, however, detect the $(FE)^{NP}$ line even at temperatures below the λ point of liquid helium. Nevertheless, a fit to Eq. (1) gives a much higher sample temperature. In the LPE samples just mentioned, apparently local heating was produced by the laser. All the samples that show this property have a high dislocation density which presumably favors local heating of the samples. The origin of this behavior is not understood at the moment.

A strong $(FE)^{NP}$ transition was reported in absorption and photoluminescence in a high-purity $Si_{1-x}Ge_x$ sample with $x=0.85$.[4] The position of this transition falls exactly at the same energy as we find for the $(FE)^{NP}$ line in a sample with the same composition.

C. Origin of the X^{NP} transition

The near-band-gap luminescence spectrum of Si-Ge alloys is dominated by the transition labeled X^{NP} in Fig. 1. From the identification of the FE lines in Sec. III B and their thermal behavior, shown in Figs. 2 and 3, we interpret the X^{NP} transitions as being due to the NP recombination of excitons bound to shallow donors and acceptors. From the energy spacing between the $(FE)^{NP}$ and the X^{NP} lines we determine the binding energy of the excitons to be about 3–6 meV. There is a large inaccuracy associated with these binding energies, due to the weakness of the FE lines in most of our samples. We are not able to establish a trend in the binding energies with composition. Possible binding centers for the excitons are boron, phosphorus, or arsenic, which have exciton binding energies in the range of 4 meV in Si and 1 meV in Ge. In a few LPE layers grown from the indium solutions, a binding energy of approximately 15 meV is derived from the spectra at higher temperatures. This value corresponds to the binding energy of the In bound exciton in Si.[19]

An Arrhenius plot of the X^{NP} line intensities gives a binding energy of ~ 5 meV, which is in agreement with the energy separation of this line from the FE line. The energetic position of the X^{NP} line is not affected by a higher sample temperature, but an increase in linewidth can be detected.

With increasing laser excitation, the line shape of the X^{NP} transition changes and a structure labeled X^{NP}_{BE} and X^{NP}_{m} in Fig. 4 can be resolved. At low excitation power the X^{NP} transition has the smallest linewidth and consists only of the X^{NP}_{BE} line. With increasing laser power the X^{NP}_{BE} line remains at the same energy position, but decreases in intensity relative to a broader band X^{NP}_{m} that emerges from the low-energy side of the X^{NP}_{BE} transition. The shift of this X^{NP}_{m} band can be as much as ~ 5 meV from the original X^{NP}_{BE} position.

In most samples, the halfwidth of the lines is too large to distinguish between these two transitions. In these cases, we detect only a shift of the X^{NP} transition and an increase of the linewidth with laser power. An example is given in Fig. 5.

The total intensity of the X^{NP} transition changes linearly with laser power in all our samples. This dependence from the laser power is shown in Fig. 6. Nonlinearities occur if we measure separately the intensity of the broad X^{NP}_{m} band and the sharper nonshifting line X^{NP}_{BE} in the samples where the X^{NP} line is structured. Whereas the intensity of X^{NP}_{m} increases almost linear with laser power, the X^{NP}_{BE} line intensity shows a sublinear depen-

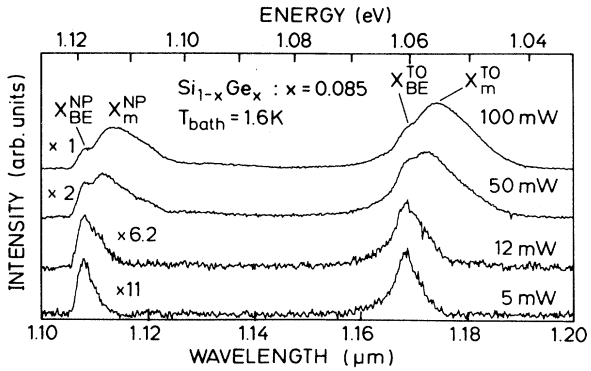

FIG. 4. Dependence of the PL spectra on laser power for sample $Si_{1-x}Ge_x$ ($x=0.085$). The excited area on the samples is approximately 1 mm^2.

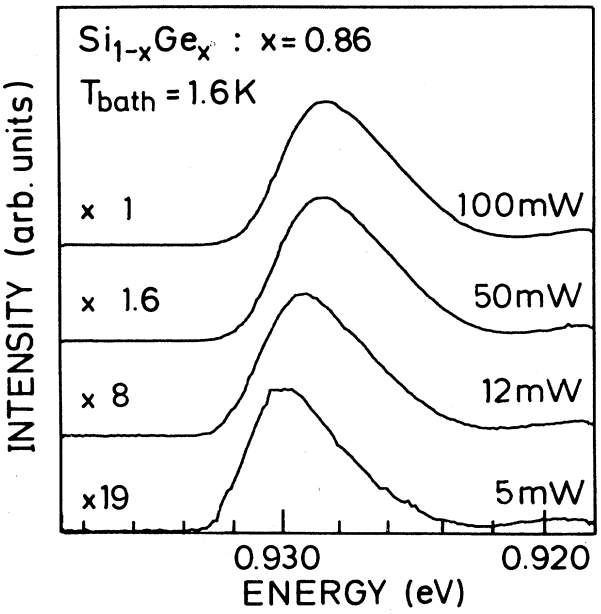

FIG. 5. Line shape of the X^{NP} transition for different laser powers. The $Si_{1-x}Ge_x$ sample has a composition of $x=0.86$. The excited area of the sample is approximately 1 mm^2.

dence, due to saturation effects.

The laser power dependence of the X^{NP} line can be understood by a bound-exciton recombination in samples with local fluctuations of the composition. Similarly, as

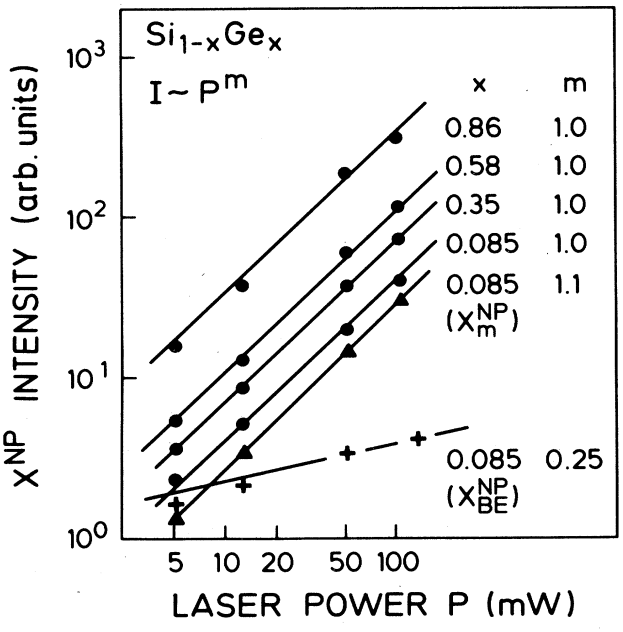

FIG. 6. Intensities of the X^{NP} transitions in different samples as a function of the laser power. For the sample with composition $x=0.085$ the intensities of X_m^{NP} (▲), X_{BE}^{NP} (+), and the total intensity X^{NP}(●) are shown.

in pure Si or Ge crystals, bound multiexciton complexes (BMEC) are formed at increased exciton densities. The decay of the BMEC's gives rise to the X_m^{NP} luminescence at the low-energy side of the bound-exciton recombination X_{BE}^{NP}. No sharp BMEC lines can be resolved in the alloy due to the increased linewidth produced by the alloy fluctuations. A similar interpretation for the long-wavelength wings of the X^{NP} lines in Si-rich alloys was proposed in Refs. 7 and 8.

D. The *L*-photoluminescence band

In several of our samples, we detect a broad luminescence band at the low-energy side of the X^{NP} transition. In Ref. 7 a band labeled L with similar properties was detected in an indium-doped $Si_{1-x}Ge_x$ sample with $x \approx 0.10$. The L band was interpreted as a bound-exciton recombination at the In acceptor. However, the unusually large temperature shift of the L-band energy could not be explained by a bound-exciton recombination process.

We detect the L band in various, differently doped samples, including those that are not deliberately doped with In. The L band is only seen at higher temperatures. In a few samples, however, we detect the L band even at low temperatures ($T=4.2$ K) as in Ref. 7, but in these samples an effective sample heating due to the laser excitation is found by a fitting of the FE line shape.

The intensity of the L band increases up to ~20 K and then decreases again. Figure 3 gives an example of the evolution of the L band with temperature. The decrease of the luminescence intensity can be explained by an ionization process of an exciton with a binding energy of $\sim 15 \pm 5$ meV. The change in linewidth of the L band is given in Fig. 7(a). At higher temperatures the linewidth of the L band shrinks and the band exhibits a symmetric shape. Temperatures higher than 40 K lead again to an increase in linewidth.

The unusual shift of the L band towards lower energies was first reported in Ref. 7. In Fig. 7(b) the nonlinear shift with temperature is shown together with the energies of the $(FE)^{NP}$ and X^{NP} luminescence. The shift of the L band seems to depend only on the quality of the sample; no influence is found from the composition x. The largest shift of ~45 meV was found in a sample with intense dislocation related luminescence bands.[17]

Our interpretation of the L band is as follows. A high-density electron-hole plasma is created in potential wells formed by large Si-Ge alloy fluctuations; perhaps in the vicinity of dislocations in these samples. The shift to lower energies that occurs at higher temperatures is then associated with the preferential formation of electron-hole plasma states in deeper potential wells. Recently, Rowell *et al.* in a PL study on molecular-beam epitaxy grown Si-Ge alloys, claim to have observed a similar alloy-induced band-to-band transition.[21] However, these authors were misled in their interpretation, since the band-gap energies of the samples were not accurately known. As we will show in Ref. 17, their alloy band coincides with dislocation related PL bands.

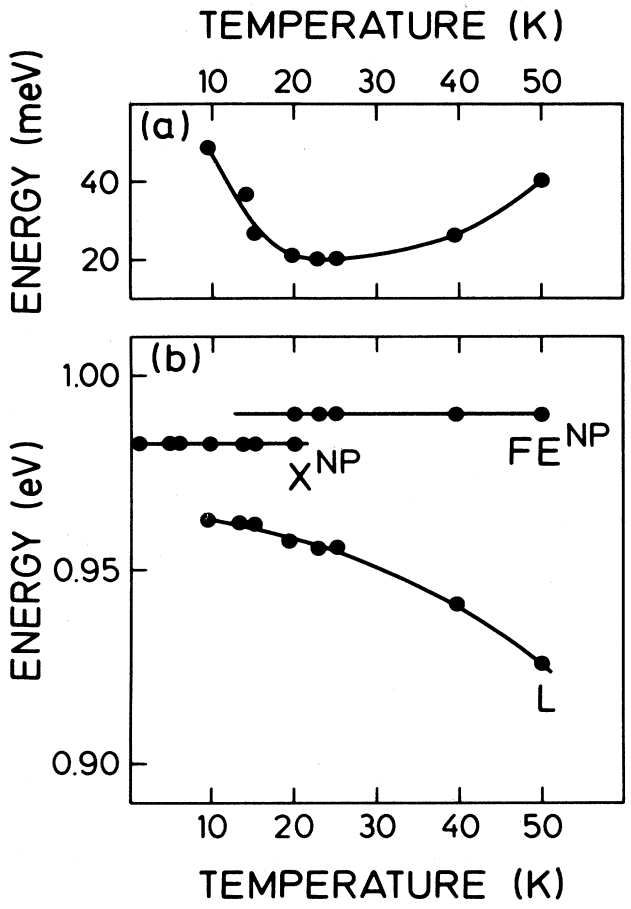

FIG. 7. (a) Temperature dependence of the L-band linewidth in sample $Si_{1-x}Ge_x$ ($x=0.58$). (b) Energy position of the PL lines in $Si_{1-x}Ge_x$ ($x=0.58$) as a function of the sample temperature.

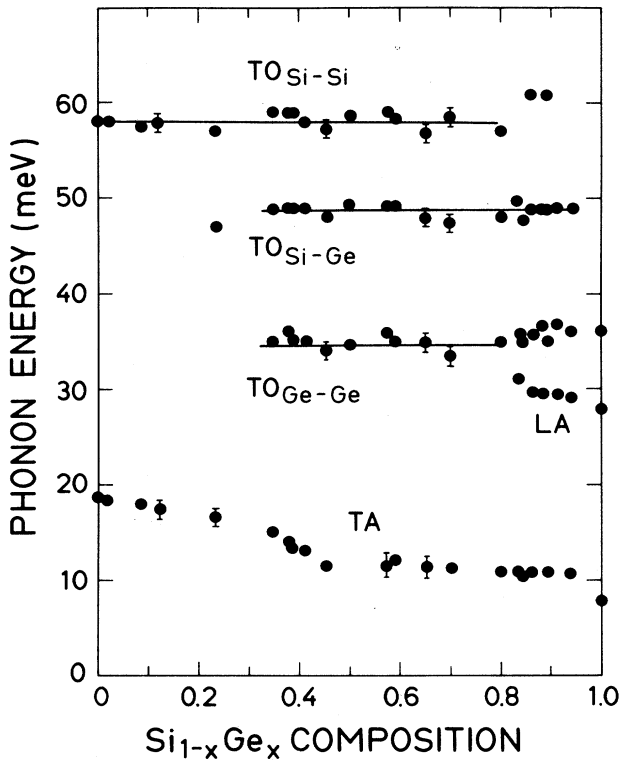

FIG. 8. Phonon energies for different compositions x derived from the energy separation between the NP lines and the phonon replica lines.

E. Phonon-assisted transitions

Several phonon-assisted optical recombination processes occur in the Si-Ge alloys in addition to the NP transitions. From the energy separation between the NP transitions and the phonon replicas, we determine the phonon energies in the alloys. In Fig. 8 we plot the observed energies of the MC phonons for different compositions.

We detect TO as well as TA phonons at the Si-rich site ($x \ll 1$) of the alloys. The linewidth of the TO-phonon replica first increases with alloying (See Fig. 1) and then splits into three separate modes at $x \sim 0.3$. We identify the three different TO-phonon lines by their energy position as due to TO-phonon vibrations of different nearest-neighbor atoms. The phonon labeled $TO_{Si\text{-}Si}$ is the momentum-conserving vibration of a Si atom surrounded by other Si atoms. Similarly, the $TO_{Ge\text{-}Ge}$ phonon is the TO-like vibration mode in Ge. Replica $TO_{Si\text{-}Ge}$ labels the vibration of a Si atom in a Ge lattice. The energy of the $TO_{Si\text{-}Ge}$ mode is almost identical to the energy one would expect for a simple harmonic oscillator with the reduced mass of a Si-Ge pair. We will show in Sec. IV B 2 that the only important parameter to describe the relative intensities of the three different TO-phonon lines is the composition x.

The phonon energies of the $TO_{Si\text{-}Si}$ and $TO_{Ge\text{-}Ge}$ phonons vary slightly for the Ge-rich alloys ($x > 0.85$). This is because, in this composition range, the electron state change from the Si-like to the Ge-like band structure and, therefore, phonons of different symmetries are needed for the momentum conservation. In Table I we summarize the observed TO-phonon energies and compare them to phonon energies of the pure Si and Ge lattices.

TABLE I. Phonon energies of TO momentum-conserving phonons in $Si_{1-x}Ge_x$ alloys.

$x<0.85$	$TO_{Si\text{-}Si}$	58.0 meV	Si: TO(Δ) (Ref. 19)
$x>0.85$	$TO_{Si\text{-}Si}$	61.0 meV	Si: TO(L_3) (Ref. 19)
$x<0.85$	$TO_{Ge\text{-}Ge}$	34.5 meV	Ge: TO(X_4) (Ref. 19)
$x>0.85$	$TO_{Ge\text{-}Ge}$	36.0 meV	Ge: TO(L_3) (Ref. 19)
$0<x<1$	$TO_{Si\text{-}Ge}$	49.0 meV	Alloy mode (Ref. 19)

Whereas the TO-phonon energies are constant with x, the TA phonons show an almost linear change with x. The TA phonons start for low x at the energy of the TA(Δ) phonon in Si. From our measurements it is not clear whether the TA-phonon energy for Ge-rich alloys coincides with the TA(X_3) or the TA(L_3) phonon energy in Ge, which are very close in energy. The LA phonon, however, merges at the Ge rich site with the LA(L_2) phonon of pure Ge. It was not possible to follow the LA-phonon replica to compositions smaller than $x \approx 0.8$.

IV. DISCUSSION

A. Determination of the indirect band gap in Si-Ge alloys

The main objective of this work is to determine the energy of the indirect band gap in Si-Ge alloys. We measured the low-temperature PL spectra of samples with different alloy composition x. As was discussed in the previous sections, we are able to analyze various optical recombination processes in the alloys. For the determination of the band-gap energy we will use the energy of the FE and BE PL lines.

In samples where the FE luminescence is detectable, we are able to obtain the FE threshold energy by a proper linefit as described in Sec. III B. The FE threshold energy determines the FE band gap in the samples at low temperatures. For all other samples, the FE band gap is calculated from the BE PL energy according to the following procedure. The BE binding energy is well known for shallow acceptors and donors in Si and Ge and is directly proportional to the acceptor or donor binding energies (Haynes rule).[22] Neglecting central cell effects, the BE binding energy is determined by the electron and hole masses and the dielectric constant of the host crystal. It is known from experimental data[23] and from calculations[24] that electron and hole masses change almost linearly in the alloy from Si to Ge. The BE binding energy for shallow donors and acceptors is ~ 5 meV for Si and ~ 1 meV in Ge.[19] We calculate the FE band-gap energy in the alloys by adding the scaled BE binding energy to the BE energy position. We estimate the error in this energy determination to be smaller than 1 meV.

The excitonic band-gap energy (E_{gx}), as determined from our PL data, as a function of the alloy composition x, is plotted in Fig. 9. The band gap varies smoothly from the Si FE gap at 1.155 eV to the excitonic gap in Ge at 0.740 eV. At around $x = 0.85$ the crossover from the Si-like X-conduction-band minimum to the Ge-like L conduction-band minimum occurs. The scatter in the data points is mainly due to the inaccuracy in the composition value x, which was discussed in Sec. II C, and is $\Delta x \approx \pm 0.015$. The scatter in the energy should not be larger than ± 0.5 meV. Therefore, the uncertainty of the data points corresponds roughly to the size of the square symbols in Fig. 9.

We fit the experimental data separately for $0 \le x < 0.85$ and $0.85 < x \le 1$ by a least-squares procedure. The analytical expressions are as follows:

$$X \text{ band: } E_{gx}^{(X)}(x) = 1.155 - 0.43x + 0.206x^2 \text{ eV} , \quad (2)$$

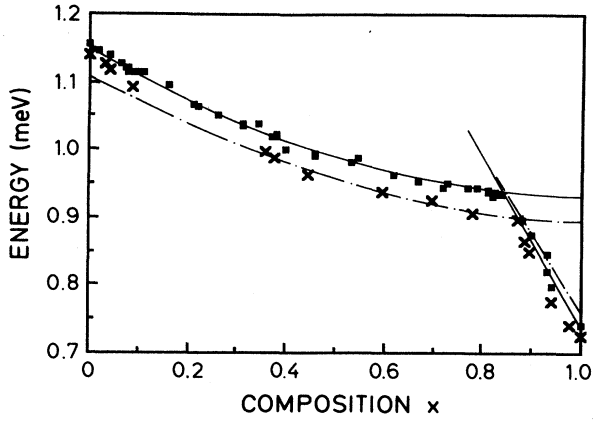

FIG. 9. Excitonic band gap (■) vs composition x for $Si_{1-x}Ge_x$ alloys, as determined from low-temperature PL spectra. Literature data are included for comparison (×) (Ref. 27). The dotted line corresponds to the analytical expression given in Ref. 33. The solid line gives our fit to the measured data.

$$L \text{ band: } E_{gx}^{(L)}(x) = 2.010 - 1.270x \text{ eV} . \quad (3)$$

The curves that fit best the experimental data [Eqs. (2) and (3)] are plotted in Fig. 9 as solid lines.

A comparison of our band gap with other published data on Si-rich and Ge-rich alloys shows remarkably good agreements. For a sample with $x = 0.11$ Mitchard *et al.* find the position of the FE 41.4 meV below the FE in pure Si.[7] This composition corresponds to a band-gap shift of 44.8 meV, according to our data. Our values of the band-gap changes are somewhat smaller than those from Ref. 8, 40.9 meV compared to 43 meV for $x = 0.1$. One has to take into account that the band-gap shift, in this case, was determined only for $0 < x < 0.1$ in Ref. 8. Safarov and Titkov find in Ge-rich alloys a change of the FE position of 12 meV per at. % Si, which corresponds to 12.7 meV in our measurements.[25]

An early absorption investigation of Si-Ge alloys for $0 < x < 1$ was performed by Johnson and Christian.[26] Their derivation of the near band gap of Si-Ge alloys is, however, far too inexact to obtain reasonable energy values.

Braunstein and co-workers, in a pioneering work, measured the optical absorption for the Si-Ge alloys system as a function of temperature and composition.[27] For several alloys the temperature-dependent energy gaps are given in Ref. 27 from 77 K up to room temperature, with the exception of pure Si and Ge, where 4.2 K data are also included. We extrapolate from Braunstein's data the energy gap at 4.2 K for the different alloy compositions. These data are given as crosses in Fig. 9.

As shown in Fig. 9, the band gaps of Si-Ge alloys determined from Ref. 27 deviate from our results. The difference in the absolute position of the band gap in pure Si and Ge by ~ 10 meV, and the much larger differences in the alloy band gaps could simply result from the inaccurate fitting process used by Braunstein *et al.*[27] In the composition range of $x \approx 0.5$ the approximation of only

one effective phonon energy is no longer valid. All three TO modes, as well as the NP transitions, have to be included in the Macfarlane-Roberts expression.[28]

Recent band-structure calculations by Krishnamurthy *et al.* of unstrained Si-Ge alloys account for the chemical and structural disorder using the molecular coherent-potential approximation (MCPA).[24] Prior authors used the virtual-crystal approximations (VCA), coherent-potential approximations (CPA), and other approximations to study the band structure and the effect of alloy disorder.[29–32] However, due to the less accurate band structures of the constituent materials involved in the alloy formalism, these calculations predict only trends of specific quantities, not quantitatively accurate results. In Ref. 33 the results of a CPA calculation are given in parametrized form for the L and X bands, respectively. The dashed lines in Fig. 9 represent the results of this calculation.

Our experimental results for $x=0$ to 0.85 are higher in energy by almost a constant amount of 0.04 eV. We feel the differences between our experimental curve and the calculated band gap result from the starting parameters, for the critical points in the band structure of pure Si or Ge, not being chosen properly in the calculation. The indirect-band-gap energies for pure Si and Ge calculated from Ref. 33 are found to be 1.11 and 0.76 eV at $T=0$ K. The exact values, which are also in agreement with the energies of our excitonic transitions, are 1.155 and 0.740 eV, respectively.[19] However, our analytical fit to the experimental data has the same curvature as the calculated band structure.

An important parameter in the band structure of alloys is the bowing parameter b, which describes the deviation from a linear band-gap shift and is identical to the prefactor of the quadratic term in Eq. (2).[34] From our analytical fit to the experimental data we find $b\approx 0.21$. The parametrized band-gap curve from the CPA calculation in Ref. 8 gives a somewhat smaller value of $b=0.18$. In the MCPA calculations, a proper account of the structural disorder due to the different bonding lengths is given.[24] According to the authors, the energy gap, compared to the CPA calculations is only slightly reduced (at $x=0.5$ by ~ 7 meV) but the bowing parameter is now $b=0.21$, identical to our measured value.

B. Effects of disorder in Si-Ge alloys

Silicon and germanium form a continuous series of substitutional solid solutions of fixed crystal structure over the entire composition range. The occupation of the substitutional lattice sites by Si or Ge is assumed to be purely statistical, although ordering effects at the Si- and Ge-rich site of the alloy were reported.[35,6] However, more recent investigations found no complexing or ordering in these unstrained bulk samples.[36] In Secs. IV B 1 and IV B 2, we discuss the influence of alloy fluctuations on the PL spectra of Si-Ge alloy samples.

1. *The linewidth of the X^{NP} transition*

The linewidth of the X^{NP} line is found to change with composition. However, as is reported in Sec. III C, the temperature and the laser power also give rise to drastic changes in the linewidth, due to the different luminescence lines $(FE)^{NP}$, X_{BE}^{NP}, and X_m^{NP} constituting the X^{NP} luminescence. From our measurements, we determine carefully the full width at half maximum (FWHM) of the X_{BE}^{NP} line by choosing the appropriate laser power and sample temperature in each case to make sure that we measure only the width of the X_{BE}^{NP} line. The results are given in Fig. 10. The linewidth of the X_{BE}^{NP} line in our best samples varies from 4 to 8 meV, with a pronounced minimum around $x=0.85$. Samples with a high dislocation density or high-impurity concentrations exhibit a much larger linewidth, and are not included in the following discussion.

The increased linewidth of the X_{BE}^{NP} transition in alloys is likely to be caused by local variations in the alloy composition x. Changes of the FE and BE binding energy and the band-gap energy with x, all contribute to the measured linewidth of X_{BE}^{NP}. The binding energies of the free and bound excitons vary linearly in the alloy as was already discussed in Sec. IV A. If we assume only small statistical fluctuations of x in our sample, we cannot account for the BE linewidth by only a change of the FE or BE binding energies with composition.

Alferov *et al.* discussed first the possibility that the linewidth broadening is the result of variations in band-gap energy produced by local fluctuations in the alloy composition x.[37] If we use their arguments, and extend the valid composition range, as was done in Ref. 38, we derive the following expression for the BE line broadening:

$$\Delta E_{BE}=2.36\left[\frac{dE_{gx}}{dx}\frac{x(1-x)}{\frac{4}{3}\pi a_B^3 N}\right]^{1/2}. \tag{4}$$

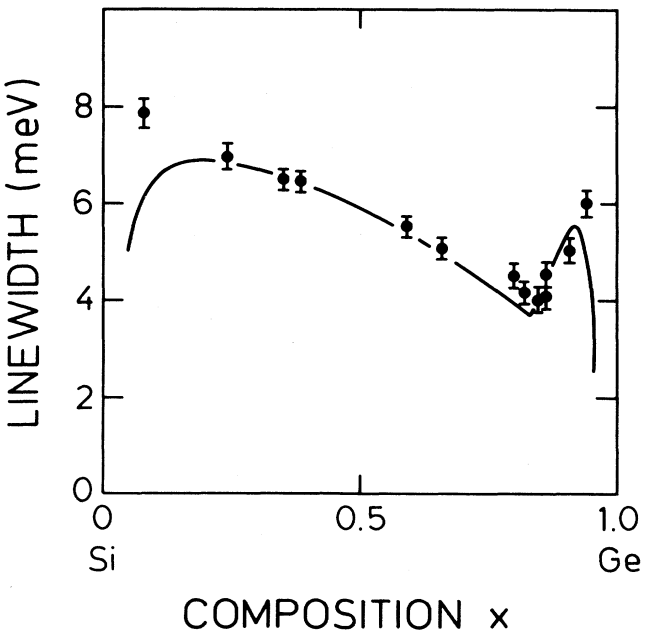

FIG. 10. Linewidth of the X_{BE}^{NP} transition vs composition. The solid line is the predicted linewidth using Eq. (4).

The derivative of the band-gap energy with respect to the composition x can be derived from the measured band gap in Sec. IV A. N is the density of lattice sites in the alloy.[7] The only adjustable parameter in this expression is the Bohr radius a_B of the bound exciton. A reasonable fit to the measured line broadenings is given in Fig. 10. We used two different Bohr radii: for $0<x<0.85$ $a_B=38$ Å, and for $0.85<x<1.0$ $a_B=110$ Å. Both values are in good agreement with the Bohr radii expected for shallow bound states in Si and Ge, respectively.[19]

In a paper by Baranovskii and Éfros[39] the binding of a FE to local fluctuations is calculated. Suslina *et al.*[30] interpret the broadening of excitonic lines in II-VI compounds according to this mechanism. In GaAsP a new PL line is identified as recombination of a FE in potential fluctuations.[41] In Si-Ge alloys Mitchard and McGill[7] find a similar excitonic recombination 0.1 meV below the FE recombination. This small binding energy leads us to believe that the binding of the FE to alloy fluctuations is not important for the linewidth of the BE lines in our samples.

Thus, the linewidth of the $X_{\mathrm{BE}}^{\mathrm{NP}}$ line in our best samples results only from the statistical fluctuations of the distribution of the Si and Ge atoms in the alloy. Additional broadening mechanisms have to account for the increased linewidth of all other samples. Possible candidates are microscopic inhomogeneities, defects, and alloy clustering.

In Ref. 8 a linear increase with x of the linewidth for $x<0.1$ was reported, and the values of the linewidth are of the same order as our measurements ($x\approx 0.1$: $\Delta E=7$ meV). Much smaller linewidths were reported by Mitchard *et al.* ($x=0.11$: $\Delta E\approx 3$ meV).[7]

We feel our increased linewidth, compared to Ref. 7, does not result from clustering in our samples. The cluster of k atoms in the alloy would increase the linewidth by a factor of $\sqrt{k}$.[35] To account for the larger linewidth in our samples, we would have to assume a clustering of 3–4 atoms in the alloy. However, from the intensity ratios of the PL lines (see Sec. IV B 2) we have no evidence for the preferential clustering of a few atoms.

2. *The relative intensities of the PL transitions*

The bound-exciton transition can occur via absorption or emission of MC phonons or with involvement of scattering centers. Due to the need of a large crystal-momentum, scattering occurs mainly by the short-range part of the impurity potential, whose spatial extent is of the order of the lattice constant.

From the PL spectra of the different Si-Ge samples (Fig. 1) it is obvious that the relative intensity of the NP transitions, compared to the phonon-assisted transition, changes with x. We plot, in Fig. 11, the intensity ratio of the NP transitions to the phonon-assisted transitions for the same set of samples used in Sec. IV B 1. The dependence on x is easily explained by the appearance of short-range potential fluctuations due to Si-Ge pairs in the alloys. The probability to find such a pair in the alloy is proportional to $x(1-x)$.[42] As shown in Fig. 11, this dependence gives a reasonable fit to the measured intensity ratios. Deviations from the curve are mainly due to the inaccurate determination of the intensities. No correction was made for the sensitivity variations of the Ge detector. The intensity ratio of the no-phonon to the phonon transitions seems to be determined only by the composition x.

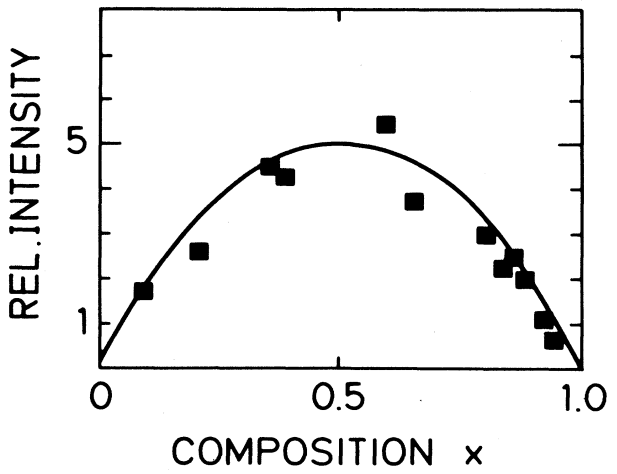

FIG. 11. Intensity ratio of the no-phonon transitions X^{NP} to the phonon replicas $X^{\mathrm{TO,LO,TA}}$ for different compositions x. The solid curve is proportional to the probability of finding a Si-Ge pair in the alloy.

There is an easy way to determine the ratio of Si and Ge atoms in the alloy from our PL spectra. As is presented in Sec. III E, and discussed in Sec. IV C, we find specific TO vibrations of Si-Si, Si-Ge, and Ge-Ge pairs in the PL spectra. The ratio of their intensities should be proportional to the number of these pairs:[11]

$$\frac{I^{\mathrm{TO}}_{(\mathrm{Ge\text{-}Ge})}}{I^{\mathrm{TO}}_{(\mathrm{Ge\text{-}Si})}}\sim\frac{(1-x)}{2x}\ , \tag{5}$$

$$\frac{I^{\mathrm{TO}}_{(\mathrm{Si\text{-}Si})}}{I^{\mathrm{TO}}_{(\mathrm{Ge\text{-}Si})}}\sim\frac{x}{2(1-x)}\ . \tag{6}$$

These ratios are calculated under the assumption of equal oscillator strengths for all pairs and a purely statistical distribution of the atoms in the alloy. In Fig. 12, we plot the intensity ratios of the different phonon lines, along with the expected dependence according to the above equations. A reasonable agreement between the experimental data and the statistical distribution is found, indicating that the occurrence of pairs is purely random and no potential ordering takes place.

C. Phonon energies in Si-Ge alloys

In general, different types of vibrational spectra are found in alloys. For some systems the phonon frequencies vary linearly with concentration and match the frequencies of the pure constituents at the ends of the concentration range. In other systems, however, vibration frequencies related to each one of the constituents can be

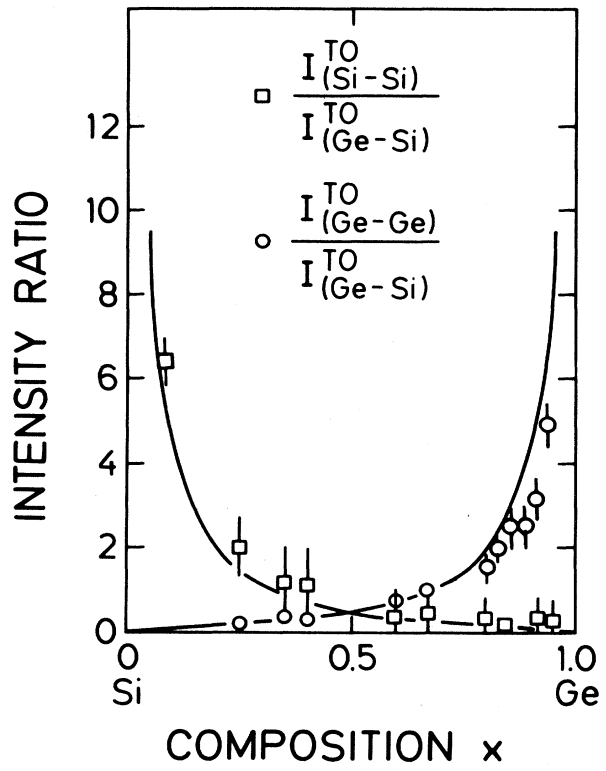

FIG. 12. Compositional dependence of the different TO-phonon line intensity ratios.

found separately, and additional frequencies of new mixed modes can occur.

In the Si-Ge alloys two types of alloy phonons can be detected. For the momentum-conserving TO phonons, we determine three different energies, which show no shift with composition x. These energies correspond to vibrations of Ge-Ge, Si-Si, and Si-Ge pairs (three-mode behavior). But an almost linear variation in x is found for the TA- and LA-phonon energies (one-mode behavior).

With a simple, one-dimensional model, Barker was able to calculate the behavior of the zone-boundary phonons in Si-Ge mixed crystals.[43] Barker finds three optical modes and only one acoustical mode. The optical modes involve the motion of only Si or Ge atoms, or a combined Si and Ge vibration, respectively. The two first-mentioned modes become the pure Si and pure Ge optic modes at $x=0$ and 1. From a more sophisticated calculation, Taylor[44] also proposes a three mode behavior of the TO phonons in Si-Ge crystals.

The frequency of the TO_{Si-Ge} vibration was calculated for zone-center phonons,[45] and measured as a local-mode vibration by infrared absorption.[46] Raman measurements give the most accurate phonon energies of the three optical modes in Si-Ge crystals.[47,48] Compared to our results, the Raman energies of the zone-center phonons show a slight dependence on x and have different energies than the MC TO phonons measured by PL.

We expect to derive the same MC TO energies from the analysis of the absorption measurements.[27] However, only one average phonon energy was used to describe the absorption process. Two phonon absorption measurements give the TO-phonon frequencies near the edge of the reduced zone,[49] but the determination of the energies is not precise enough to compare them with the PL data.

The one-mode behavior of the acoustic phonons is explained in Ref. 27 by the virtual-crystal and ordered-crystal approximations. According to these models, the MC phonons should vary linearly with composition in the $x=0.85-1.0$ range [(111) phonons] and in the $x=0-0.85$ range [(100) phonons]. At $x\sim0.85$ a slight discontinuity in energy is expected due to the change over from (111) to (100) phonons. The (111) and the (100) LA and TA phonons have nearly the same energies at this composition and we expect that the indirect electronic transitions take place both at the (100) and (111) conduction-band minima.

In PL measurements the MC TO_{Si-Ge} phonon was first reported in Ge-rich alloys.[5] This phonon couples to the BE and FE recombination. We find the same behavior in our samples. Benoit à la Guillaume *et al.* report on PL measurements on a sample of $Si_{0.15}Ge_{0.85}$.[4] In their spectra the FE, as well as the electron-hole droplet (EHD), recombination couples to the TO_{Si-Ge} mode.

V. CONCLUSION

In the paper we have presented a detailed study of the near-band-gap PL in $Si_{1-x}Ge_x$ with composition x ranging from 0 to 1. Several excitonic recombination processes have been identified and typical features in the alloys have been discussed. The linewidth of the BE recombination and the intensity ratios of the different lines can be described under the assumption of a purely statistical disorder in the alloys. We determined the energies of the momentum conserving phonons and the band-gap energy in the alloys.

ACKNOWLEDGMENTS

The authors are grateful to M. Cardona, K. Holm, and K. Wang for the loan of several Si-Ge alloy samples. The guidance of E. Bauser, during the LPE growth, is highly appreciated. We thank W. Heinz and W. Krause for technical assistance with the photoluminescence measurements, and M. Garriga for the ellipsometry measurements. We are indebted to M. Cardona and H. J. Queisser for fruitful discussions, continuing encouragement, and support.

[1]C. Abstreiter, H. Brugger, T. Wolf, H. Jorke, and H. J. Herzog, Phys. Rev. Lett. **54**, 2441 (1985).
[2]T. P. Pearsall, J. Berk, L. C. Feldman, J. M. Bonar, and J. P. Mannaerts, Phys. Rev. Lett. **58**, 729 (1987).
[3]K. Eberl, G. Krötz, R. Zachai, and G. Abstreiter, J. Phys. (Paris) Colloq. **48**, C5-329 (1987).
[4]C. Benoit à la Guillaume, M. Voos, and Y. Pétroff, Phys. Rev. B **10**, 4995 (1974).
[5]E. F. Gross, N. S. Sokolov, and A. N. Titkov, Fiz. Tverd. Tela **14**, 2004 (1972) [Sov. Phys.—Solid State **14**, 1732 (1973)].
[6]R. Rentzsch and I. S. Shlimak, Fiz. Tekh. Poluprovodn. **12**, 713 (1978) [Sov. Phys.—Semicond. **12**, 416 (1978)].
[7]G. S. Mitchard and T. C. McGill, Phys. Rev. B **25**, 5351 (1982).
[8]A. S. Lyutovich, K. L. Lyutovich, V. P. Popov, and L. N. Safronov, Phys. Status Solidi B **129**, 313 (1985).
[9]J. P. Dismukes, L. Ekstrom, and R. J. Paff, J. Phys. Chem. **68**, (1964) 3021.
[10]J. S. Kline, F. H. Pollak, and M. Cardona, Helv. Phys. Acta **41**, 968 (1968).
[11]M. A. Renucci, J. B. Renucci, and M. Cardona, in *Light Scattering in Solids,* edited by M. Balkanski (Flammarion, Paris, 1971), p. 326.
[12]M. I. Alonso and E. Bauser, J. Appl. Phys. **62**, 4445 (1987).
[13]C. Holm and E. Sirtl, J. Cryst. Growth **54**, 253 (1981).
[14]F. Cerdeira, A. Pinczuk, J. C. Bean, B. Batlogg, and B. A. Wilson, Appl. Phys. Lett. **45**, 1138 (1984).
[15]J. Humlíček, M. Garriga, M. I. Alonso, and M. Cardona, J. Appl. Phys. **65**, 2827 (1989).
[16]M. I. Alonso, E. Bauser, T. Suemoto, and M. Garriga, in *Proceedings of the 18th International Conference on the Physics of Semiconductors,* edited by O. Engström (World Scientific, Singapore, 1987), Vol. 1, p. 771.
[17]J. Weber and M. I. Alonso (unpublished).
[18]P. J. Dean, J. R. Haynes, and W. F. Flood, Phys. Rev. **161**, 711 (1967).
[19]*Numerical Data and Functional Relationships in Science and Technology,* Vols. 17(a) and 17(b) of *Landolt-Börnstein,* edited by O. Madelung (Springer-Verlag, Berlin, 1982).
[20]S. A. Lyon, D. L. Smith, and T. C. McGill, Phys. Rev. Lett. **41**, 56 (1978).
[21]N. L. Rowell, J. M. Baribeau, and D. C. Houghton, J. Electrochem. Soc. **135**, 2843 (1988).
[22]J. R. Haynes, Phys. Rev. Lett. **4**, 361, (1960).
[23]R. Braunstein, Phys. Rev. **130**, 869 (1963).
[24]S. Krishnamurthy, A. Sher, and A.-B. Chen, Phys. Rev. B **33**, 1026 (1986).
[25]V. I. Safarov and A. N. Titkov, Fiz. Tverd. Tela **14**, 458 (1972) [Sov. Phys.—Solid State **14**, 380 (1972)].
[26]E. R. Johnson and S. M. Christian, Phys. Rev. **95**, 560 (1954).
[27]R. Braunstein, A. R. Moore, and F. Herman, Phys. Rev. **109**, 695 (1958).
[28]G. G. Macfarlane and V. Roberts, Phys. Rev. **97**, 1714 (1955).
[29]D. Stroud and H. Ehrenreich, Phys. Rev. B **2**, 3197 (1970).
[30]D. J. Stukel, Phys. Rev. B **3**, 3347 (1971).
[31]M. Podgorny, G. Wolfgarten, and J. Pollmann, J. Phys. C **19**, L141 (1986).
[32]B. K. Agrawal, Phys. Rev. B **22**, 6294 (1980).
[33]S. Krishnamurthy, A. Sher, and A.-B. Chen, Appl. Phys. Lett. **47**, 160 (1985).
[34]J. A. Van Vechten and T. K. Bergstresser, Phys. Rev. B **1**, 3351 (1970).
[35]I. S. Shlimak, A. L. Éfros, and I. Ya. Yanchev, Fiz. Tekh. Poluprovodn. **11**, 257 (1977) [Sov. Phys.—Semicond. **11**, 149 (1977)].
[36]A. Qteish, and R. Resta, Phys. Rev. B **37**, 1308 (1988).
[37]Zh. I. Alferov, E. L. Portnoi, and A. A. Rogachev, Fiz. Tekh. Poluprovodn. **2**, 1194 (1969) [Sov. Phys.—Semicond. **2**, 1001 (1969)].
[38]E. F. Schubert, E. O. Göbel, Y. Horikoshi, K. Ploot, and H. J. Queisser, Phys. Rev. B **30**, 813 (1984).
[39]D. S. Baranovskii and A. L. Éfros, Fiz. Tekh. Poluprovodn. **12**, 2233 (1978) [Sov. Phys.—Semicond. **12**, 1328 (1978)].
[40]L. G. Suslina, A. G. Plyukhin, D. L. Fedorov, and A. G. Areshkin, Fiz. Tekh. Poluprovodn. **12**, 2238 (1978) [Sov. Phys.—Semicond. **12**, 1331 (1978)].
[41]Shui Lai and M. V. Klein, Phys. Rev. Lett. **44**, 1087 (1980).
[42]A. N. Pikhtin, Fiz. Tekh. Poluprovodn. **11**, 425 (1977) [Sov. Phys.—Semicond. **11**, 245 (1977)].
[43]A. S. Barker, in *Localized Excitations in Solids,* edited by R. F. Wallis (Plenum, New York, 1968), p. 581.
[44]D. W. Taylor, Phys. Rev. B **156**, 1017 (1967).
[45]G. Lucovsky, M. H. Brodsky, and E. Burstein, Phys. Rev. B **2**, 3295 (1970).
[46]A. E. Cosand and W. G. Spitzer, J. Appl. Phys. **42**, 5241 (1971).
[47]D. W. Feldman, M. Ashhin, and J. H. Parker, Jr., Phys. Rev. Lett. **17**, 1209 (1966).
[48]M. I. Alonso and K. Winer, Phys. Rev. B **39**, 10056 (1989).
[49]R. Braunstein, Phys. Rev. **130**, 879 (1963).